

# Thermochemical Modeling of Glass: Application to High-Level Nuclear Waste Glass

Karl E. Spear, Theodore M. Besmann, and  
Edward C. Beahm

---



PENNSSTATE

---



Reprinted from Materials Research Society  
*MRS Bulletin*, Volume 24, Number 4  
April 1999

MRS

BULLETIN

# Thermochemical Modeling of Glass: Application to High-Level Nuclear Waste Glass

Karl E. Spear, Theodore M. Besmann, and Edward C. Beahm

## Introduction

Despite the obvious importance of understanding the chemistry of oxide glass materials, predictive thermochemical models of complex glasses have not yet been developed. Such models are important for technologies such as the disposal of high-level nuclear and transuranic waste (HLW), which are currently foreseen as being incorporated in a host glass for permanent sequestration. A large number of glasses have been explored, with a borosilicate glass being the typical base composition. An example of the complexity of such a HLW glass is given in Table I. This article discusses our attempts to develop an accurate, easy to understand and use glass solution model for describing the thermodynamic stability of such HLW glasses. Critical for such a model is the availability of reliable thermodynamic data that can be used in generating accurate values for thermodynamic activities of glass components as a function of temperature and glass composition. Therefore, a major part of this article focuses on developing reliable sets of thermodynamic data for complex HLW glass systems and subsystems. With such information and a model, we can make predictions of the stability of these waste forms, including their volatility, leaching behavior, and corrosion reactions, and understand crystallization behavior during both the initial glass processing and long-term storage.

Using an equilibrium thermodynamic model is often questioned, since HLW is

to be stored as part of a glass phase, and glass is a nonequilibrium material. Our model uses a pseudoequilibrium approach in which we thermochemically treat the glass as a supercooled liquid. This is a more accurate approach than assuming a global system equilibrium, as it describes the behavior of the metastable glass phase using thermodynamic

data for the liquid phase and excludes the formation of crystalline species. As a result, developing an accurate model and data for representing the thermodynamic properties of oxide liquid phases is critical to understanding the limiting chemical behavior of the nuclear waste glass.

The methodology requires that a critically assessed thermodynamic database be created for binary and ternary combinations of the major constituents in a typical waste glass. These data can then be combined to represent the thermodynamic behavior of the more complex multicomponent HLW glass systems. If a crystalline phase is experimentally observed to precipitate from the glass under certain conditions, a thermodynamic description can be used to calculate the composition-temperature conditions under which this specific crystalline phase can exist in equilibrium with the metastable glass phase. The change in glass phase composition immediately adjacent to the precipitated crystals can also be calculated and the properties of this new composition contrasted with that of the bulk glass.

A major concern with radioactive-waste storage is the possibility of active components leaching from the waste should it come into contact with groundwater. Accurate predictions of leaching from a chemically complex nuclear waste glass require accurate thermodynamic activities of its component oxides. However, these have not been generally

Table I: An Example of Components in High-Level Nuclear Waste Glass.<sup>1</sup>

Major	mol%	Trace	mol%
SiO <sub>2</sub>	54.82	U <sub>3</sub> O <sub>8</sub>	0.167
Li <sub>2</sub> O	9.66	ThO <sub>2</sub>	0.047
Na <sub>2</sub> O	9.24	Cr <sub>2</sub> O <sub>3</sub>	0.052
B <sub>2</sub> O <sub>3</sub>	7.55	CuO	0.363
Fe <sub>2</sub> O <sub>3</sub>	2.86	CaSO <sub>4</sub>	0.037
FeO	2.84	BaSO <sub>4</sub>	0.116
K <sub>2</sub> O	2.69	NaCl	0.213
Al <sub>2</sub> O <sub>3</sub>	2.56	Na <sub>2</sub> SO <sub>4</sub>	0.055
MgO	2.20	Subtotal trace	1.050
MnO	1.88	Others	
CaO	1.13	Group A	
NiO	0.78	Tc, Se, Te, Rb, Mo	
TiO <sub>2</sub>	0.74	Group B	
Subtotal major	98.95	Ag, Cd, Cr, Pd, Tl, La, Ce, Pr, Pm, Nd, Sm, Sn, Sb, Co, Zr, Nb, Eu, Np, Am, Cm	

available to date, and over-simplistic assumptions for the activities of glass components or correlations of the free energy of hydration with the bonding of the glass constituents are currently being incorporated in most leaching predictions.<sup>2</sup> Figure 1 schematically illustrates the critical dependence of leachate concentrations on the assumptions about the thermodynamic activities of metal oxide constituents in the glass.

## Developing Reliable Thermodynamic Data Sets

A major focus of our efforts to thermochemically describe glass—and HLW glass systems in particular—has been to develop internally consistent sets of thermochemical information for major binary and ternary subsystems of the glass. Our approach has involved the “thermodynamic fitting of equilibrium phase diagrams” as a means of testing and generating thermodynamic information for glass-forming oxide systems. Since a phase diagram graphically depicts the equilibrium chemistry and thermodynamic properties of a system, the diagram can be calculated if the thermodynamic properties are known for all chemical species/phases that can form in the system.

The computer program ChemSage™ is our primary tool for developing an assessed, internally consistent thermodynamic database and for subsequent calculations of the equilibrium chemical behavior of the glass systems.<sup>3</sup> The needed thermodynamic data are obtained from the literature and sources such as the assessed Scientific Group Thermodata Europe (SGTE) database,<sup>4</sup> our estimates, and simultaneously comparing and optimizing sets of phase equilibria and thermodynamic data. A primary source of phase-diagram information is the set of volumes *Phase Diagrams for Ceramists*,<sup>5</sup> plus literature which includes reports of previously optimized thermochemical data; recent typical examples are from Eriksson, Wu, and Pelton.<sup>6–8</sup> Since we use a different liquid solution model in our assessments and calculations<sup>9</sup> than those used in most reported studies, the literature information for liquid solutions is used only for comparison with our assessments.

A large fraction of the needed thermochemical information has not been measured or reported, so we have developed a set of procedures for estimating or calculating the information. In all cases, the complete set of thermochemical information for a system is refined and tested to give reasonable thermodynamic and

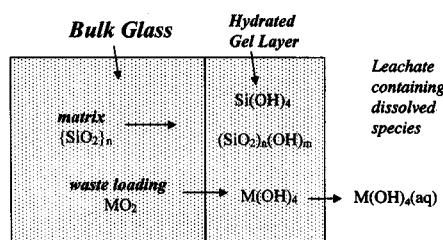


Figure 1. Schematic of the leaching process, where  $MO_2$  is a waste metal oxide in the glass. The equilibrium concentration of the leached waste species,  $M(OH)_4(aq)$ , is dependent on the activity of the  $MO_2$  in the glass.

phase-diagram information over wide ranges of temperature and compositions.

The thermodynamic information needed for each solid, liquid, and gaseous species in our high-level nuclear waste glass systems includes

- 298 K enthalpy of formation,  $\Delta H_{f,298}^0$ .
- 298 K absolute entropy,  $S_{298}^0$ .
- Heat-capacity relations from 298 K to the highest temperature of interest:  $C_p(298 - T_{tr1})$ , with phase-transformation temperature  $T_{tr1}$  and enthalpy  $\Delta H_{T_{tr1}}^0$ ;  $C_p(T_{tr2} - T_{tr1})$ , with phase-transformation temperature  $T_{tr2}$  and enthalpy  $\Delta H_{T_{tr2}}^0$ ; etc.

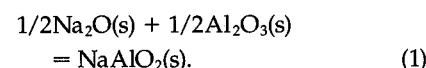
For each chemical system being evaluated, we first search for available assessed data, initially in the SGTE database.<sup>4</sup> If data are not available from this or other sources, or are incomplete, we estimate values needed for an internally consistent data set via optimization of a phase diagram and the thermodynamic data. The optimization process for a chemical system tests the total set of system data for internal consistency. Due to the extreme sensitivity of the phase equilibria to the thermochemical values, even phase-diagram uncertainties of 50–100 K in melting temperatures of some phases would yield uncertainties of only a few kilojoules in the relative stabilities of the corresponding phases. In other words, a phase diagram places very restrictive limits on the relative thermodynamic stabilities of phases in a system.

For the ceramic systems of importance for high-level nuclear waste glass, we frequently have to estimate fusion enthalpies and entropies, enthalpies of formation at 298 K, absolute entropies at 298 K, and  $C_p$  equations for temperatures from 298 K to 3000 K and higher. We use trends in chemical-reaction values as described by Spear<sup>10</sup> for entropies and heat capacities, and then use the forced fitting of phase

diagrams for generating enthalpy of formation values. As an example, we have developed what we believe is a reliable set of data for the  $Na_2O-Al_2O_3$  system. A search of the SGTE database<sup>4</sup> and other sources for the  $Na_2O-Al_2O_3$  system revealed a lack of values for the fusion of  $NaAlO_2$ , and no thermodynamic data for  $\beta''-Al_2O_3$  [ $Na_2O \cdot 6Al_2O_3$ ] and  $\beta-Al_2O_3$  [ $Na_2O \cdot 11Al_2O_3$ ]. We estimated fusion enthalpies and entropies, absolute entropies at 298 K, and  $C_p$  equations for temperatures from 298 K to 3000 K, and calculated enthalpies of formation at 298 K by developing an internally consistent set of phase-diagram and thermodynamic data. This set of data is shown in Table II and was used to calculate the diagrams in Figures 2a and 2b. The values in Table II shown in italics and underlined were estimated or calculated during the optimization process. In general, entropies are estimated and enthalpies of reaction are derived from the phase equilibria.

To illustrate some of the basic assumptions we use when estimating the initial set of thermodynamic data for a given system, we will use the  $Na_2O-Al_2O_3$  system. Initial estimates may be adjusted during the course of an evaluation in order to obtain an internally consistent set of phase-diagram and thermodynamic information, but these adjustments are not allowed to produce values outside limits that are reasonable for a specific property of a system.

Consider the following solid-state chemical reaction:



In estimating thermodynamic data for such reactions, we have found that the approximation

$$\Delta C_p = 0 \quad (2a)$$

(we use the general equation

$$C_p = a + bT + cT^2 + d/T^2) \quad (2b)$$

or

$$C_p[NaAlO_2(s)] = \frac{1}{2}C_p[Na_2O(s)] + \frac{1}{2}C_p[Al_2O_3(s)] \quad (2c)$$

is quite reasonable. In our current research on high-level nuclear waste, we are generally interested in free energies and their associated equilibrium constants. The following equations show that uncertainties in enthalpy and entropy changes that occur as a result of the assumption  $\Delta C_p = 0$  largely cancel out in the free-energy equation.

$$\Delta G_T^0 = \Delta H_T^0 - T\Delta S_T^0 = -RT \ln K_{eq} \quad (3a)$$

$$\Delta H_T^0 = \Delta H_{298}^0 + \int_{298}^T (\Delta C_p) \delta T \quad (3b)$$

$$\Delta S_T^0 = \Delta S_{298}^0 + \int_{298}^T (\Delta C_p/T) \delta T \quad (3c)$$

$$\Delta G_T^0 = \Delta H_{298}^0 - T\Delta S_{298}^0 + \left\{ \int_{298}^T (\Delta C_p) \delta T - T \int_{298}^T (\Delta C_p/T) \delta T \right\} = -RT \ln K_{eq} \quad (3d)$$

The assumption that

$$\Delta S_{298}^0 = 0 \quad (4a)$$

or

$$S_{298}^0[\text{NaAlO}_2(\text{s})] = 1/2 S_{298}^0[\text{Na}_2\text{O}(\text{s})] + 1/2 S_{298}^0[\text{Al}_2\text{O}_3(\text{s})] \quad (4b)$$

for solid-state reactions such as the one given in Equation 1 has also been shown to be quite reasonable,<sup>10</sup> yielding uncertainties of no more than a few J/K. With a more detailed study of specific classes of materials, and of trends with periodicity, the entropies can be predicted with an even higher accuracy.

Entropies of fusion can also be estimated very well, which is not surprising,

since the phase transformation from an ordered crystalline oxide phase to a disordered liquid would be expected to be fairly independent of the chemical nature of the oxide.<sup>10</sup> If data are not available for intermediate compounds, such as for NaAlO<sub>2</sub>(s), then a compositionally weighted average of the two end-member components is used. For example, the  $\Delta S_{T_{\text{fus}}}^0$  for NaAlO<sub>2</sub>(s) was assumed equal to one-half the value for Na<sub>2</sub>O plus one-half the value for Al<sub>2</sub>O<sub>3</sub>. The relationship of

$$\Delta S_{T_{\text{fus}}}^0 = (\Delta H_{T_{\text{fus}}}^0 / T_{\text{fus}}) \quad (5)$$

Table II: An Optimized Thermodynamic Data Set for the Condensed Na<sub>2</sub>O-Al<sub>2</sub>O<sub>3</sub> System.\*

(a) Crystalline Species Formulae Written with the Moles of (Na + Al) = 2

	<i>n</i> (Na <sub>2</sub> O)	<i>n</i> (Al <sub>2</sub> O <sub>3</sub> )	$-\Delta H_{f,298}$ (J/mol)	<i>S</i> <sub>298</sub> (J/K-mol)	<i>T</i> <sub>fus</sub> (K)	$\Delta H_{\text{fus}}$ (J/mol)	$\Delta S_{\text{fus}}$ (J/K-mol)
Na <sub>2</sub> O	1.000	0.000	417,982	75.04	1405	47,698	33.95
NaAlO <sub>2</sub>	0.500	0.500	1,133,090	70.40	1923	<u>78,543</u>	<u>40.84</u>
Na <sub>2</sub> Al <sub>12</sub> O <sub>19</sub> ;/7	0.143	0.857	<u>1,528,335</u>	<u>56.31</u>	1833	peritectoid decomposition	
Na <sub>2</sub> Al <sub>22</sub> O <sub>34</sub> ;/12	0.083	0.917	<u>1,593,800</u>	<u>54.18</u>	2273	<u>105,901</u>	<u>46.59</u>
Al <sub>2</sub> O <sub>3</sub>	0.000	1.000	1,675,690	50.94	2325	111,085	47.74

(b) Liquid Species Formulae Written with the Moles of (Na + Al) = 2

	<i>n</i> (Na <sub>2</sub> O)	<i>n</i> (Al <sub>2</sub> O <sub>3</sub> )	$-\Delta H_{f,298}$ (J/mol)	<i>S</i> <sub>298</sub> (J/K-mol)
Na <sub>2</sub> O(l)	1.000	0.000	370,284	108.99
NaAlO <sub>2</sub> (l)	0.500	0.500	<u>1,054,547</u>	<u>111.24</u>
Al <sub>2</sub> O <sub>3</sub> (l)	0.000	1.000	1,564,605	98.68

(c) Heat Capacity Coefficients:  $C_p = a + bT + cT^2 + d/T^2$  (J/K-mol)

Crystal Species	<i>a</i>	<i>b</i>	<i>c</i>	<i>d</i>	<i>T</i> <sub>trans</sub> (K)	$\Delta H_{\text{trans}}^0$ (J/mol)
Na <sub>2</sub> O(s)	55.480	7.021E-2	-3.054E-5	-414,000	1023	1,757.3
	82.563	1.235E-2	0	0	1243	11,924.4
	82.563	1.235E-2	0	0	2500	—
NaAlO <sub>2</sub> (s)	<u>86.485</u>	<u>4.030E-2</u>	<u>-1.527E-5</u>	<u>-2,062,500</u>	<u>1000</u>	<u>0**</u>
	<u>100.027</u>	<u>1.127E-2</u>	<u>0</u>	<u>-1,855,500</u>	<u>2500</u>	—
Na <sub>2</sub> Al <sub>12</sub> O <sub>19</sub> ;/7	<u>108.631</u>	<u>1.893E-2</u>	<u>-4.363E-6</u>	<u>-3,240,000</u>	<u>1000</u>	<u>0</u>
	<u>112.500</u>	<u>1.066E-2</u>	<u>0</u>	<u>-3,180,857</u>	<u>3000</u>	—
Na <sub>2</sub> Al <sub>22</sub> O <sub>34</sub> ;/12	<u>112.323</u>	<u>1.537E-2</u>	<u>-2.546E-6</u>	<u>-3,436,250</u>	<u>1000</u>	<u>0</u>
	<u>114.579</u>	<u>1.054E-2</u>	<u>0</u>	<u>-3,401,750</u>	<u>3000</u>	—
Al <sub>2</sub> O <sub>3</sub> (s)	117.490	1.038E-2	0	-3,711,000	3000	—
Liquid Species	<i>a</i>	<i>b</i>	<i>c</i>	<i>d</i>	<i>T</i> <sub>trans</sub> (K)	$\Delta H_{\text{trans}}^0$ (J/mol)
Na <sub>2</sub> O(l)	55.480	7.021E-2	-3.054E-5	-414,000	1023	1,757.3
	82.563	1.235E-2	0	0	1243	11,924.4
	82.563	1.235E-2	0	0	1405	fusion
	104.600	0	0	0	3000	—
NaAlO <sub>2</sub> (l)	<u>86.485</u>	<u>4.030E-2</u>	<u>-1.527E-5</u>	<u>-2,062,500</u>	<u>1000</u>	<u>0</u>
	<u>100.027</u>	<u>1.127E-2</u>	<u>0</u>	<u>-1,855,500</u>	<u>1923</u>	fusion
	<u>148.532</u>	<u>0</u>	<u>0</u>	<u>0</u>	<u>3000</u>	—
Al <sub>2</sub> O <sub>3</sub> (l)	117.490	1.038E-2	0	-3,711,000	2325	fusion
	192.464	0	0	0	3000	—

\*Values in italics and underlined were estimated or calculated during the optimization process.

\*\*A value of zero for the enthalpy of transition indicates no transition occurs, but a new *C<sub>p</sub>* equation is used for the next temperature range.

at the congruent melting point of a phase ( $\Delta G_{fus}^0 = 0$ ) then provides us with enthalpy of fusion values. If the estimated entropy of fusion is in error, the enthalpy of fusion will include this error, but the predicted melting temperature is forced to be correct by Equation 5.

### Description of Liquid Solution Model Used for Glass

Since we consider HLW glass as a supercooled liquid phase, modeling oxide liquid solutions is of critical importance to our thermodynamic description of the glass. We have chosen to develop and use an associate-species model for these liquid solutions. The associate-species solution model uses intermediate "chemical species," with their corresponding thermodynamic data, to represent the negative, nonideal mixing of the end-member components in a system. For example, a liquid  $\text{NaAlO}_2(\text{l})$  species is ideally mixed with end-member  $\text{Na}_2\text{O}(\text{l})$  and  $\text{Al}_2\text{O}_3(\text{l})$  to represent the liquid phase in the  $\text{Na}_2\text{O}-\text{Al}_2\text{O}_3$  binary system. While  $\text{NaAlO}_2(\text{l})$  may not exist as a chemical entity that can be isolated and characterized, this species in the model can accurately represent the negative interaction energies that occur between sodium and aluminum in an oxide liquid solution.

The associate-species model was first expanded for complex solutions by Hastie, Bonnell, and co-workers<sup>11-14</sup> in the 1980s in an attempt to thermodynamically describe slag systems. A review of much of their research incorporating this model is given in Bonnell and Hastie.<sup>14</sup> Pantano, Spear, and co-workers used the model for predicting and explaining interface reactions in fiber-reinforced, glass-matrix composite systems,<sup>15,16</sup> and the behavior of tin and iron in float-glass systems.<sup>17,18</sup> Other models have been used to represent the thermodynamic properties of nuclear waste glass, the most notable being the modified quasichemical model developed by Pelton, Blander, and co-workers<sup>19,20</sup> to successfully represent molten slag phases and, later, nuclear materials, including waste glass.<sup>21</sup>

We are using the associate-species model for our liquid solutions because we believe it will (1) accurately represent the thermodynamic behavior of very complex chemical systems over wide temperature and composition ranges, (2) accurately predict the activities of components in metastable equilibrium glass phases, (3) make it possible for us to logically estimate unknown thermodynamic values with an accuracy greater than that required for predicting useful engineering limits on thermodynamic

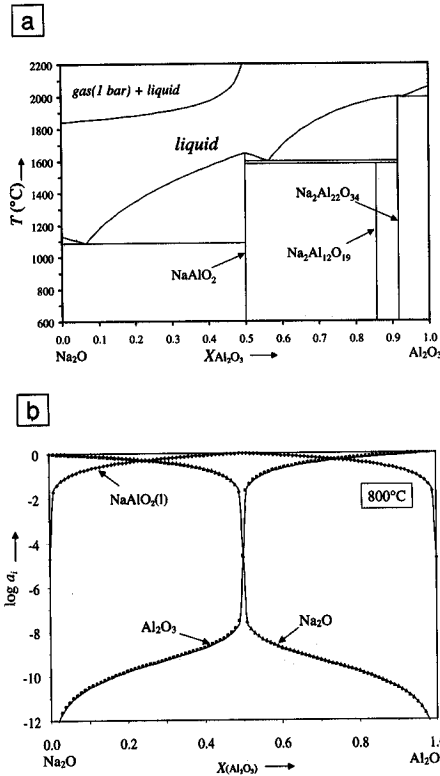


Figure 2. (a) Calculated phase diagram for the  $\text{Na}_2\text{O}-\text{Al}_2\text{O}_3$  system using ChemSage™,<sup>3</sup> optimizing the thermodynamic data for the liquid phase to reproduce the melting temperatures<sup>5</sup> of the stoichiometric compound phases. (b) Calculated activities  $a_i$  of  $\text{Na}_2\text{O}$ ,  $\text{Al}_2\text{O}_3$ , and  $\text{NaAlO}_2$  supercooled liquid species at  $800^\circ\text{C}$  for a  $\text{Na}_2\text{O}-\text{Al}_2\text{O}_3$  glass system using the thermodynamic data that produced the phase diagram in Figure 2a. The formation of equilibrium crystalline phases was suppressed.

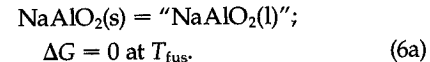
activities in solutions, and (4) be easy for nonspecialists in thermochemistry to understand and use. Our experience to date with this model has been quite positive, and although it is not the answer to all thermodynamic solution problems, it is working very well with the HLW oxide systems.

Solution interactions in which end-member component oxides exhibit neutral-to-strong attractive associations can be effectively treated with the associate-species model. In the case of strong associations, a very stable associate species is needed. When the bulk liquid composition is the same as that of the associate species, this single species dominates the liquid composition so that the ideal mixing term is not a factor in determining the stability of this par-

ticular liquid composition. Such behavior is exemplified in Figure 2b with the  $\text{NaAlO}_2(\text{l})$  associate species. Positive interactions (repulsion terms ultimately leading to miscibility gaps) cannot be modeled using the associate-species model, but we can use a positive, regular solution constant between liquid associate species bounding the composition region in which repulsive interactions occur.

In using the associate-species model to represent the thermodynamic properties of the liquid phase in the  $\text{Na}_2\text{O}-\text{Al}_2\text{O}_3$  binary oxide system, we created an ideal liquid solution phase from end-member liquid components  $\text{Na}_2\text{O}(\text{l})$  and  $\text{Al}_2\text{O}_3(\text{l})$ , and an intermediate  $\text{NaAlO}_2(\text{l})$  associate liquid species. In calculating the equilibrium state of these three liquid species in the liquid phase, the minimization of the total free energy determines the relative mole fractions of the species. Since the system is treated as an ideal solution, the activities of these species are by definition equivalent to their mole fractions, and these activities can be used to predict leaching behavior, corrosion reactions, and other important phenomena.

The free energy of formation of the associate species,  $\text{NaAlO}_2(\text{l})$ , is readily obtained from considerations of the congruent melting reaction

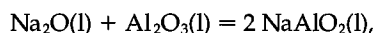


Thus at  $T_{\text{fus}}$

$$\Delta G_f[\text{NaAlO}_2(\text{s})] = \Delta G_f^0[\text{NaAlO}_2(\text{s})] = \Delta G_f[\text{"NaAlO}_2(\text{l})\text{"}]. \quad (6b)$$

The free energy and standard free energy of formation of the solid are identical since the pure stoichiometric solid phase is defined as having unit activity. The same may not be true for the liquid phase in equilibrium with this solid. The "NaAlO<sub>2</sub>(l)" liquid solution phase is written within quotation marks because the liquid solution is composed of  $\text{Na}_2\text{O}$ ,  $\text{Al}_2\text{O}_3$ , and  $\text{NaAlO}_2$  liquid species, with a constraint that the liquid composition be identical to that of the solid-phase composition in Equation 6a at the congruent melting temperature. The relative amount of each liquid species can be represented by its mole fraction  $Y_i$ . As mentioned above, these mole-fraction terms are equal to the activities of the liquid species,  $a_i = Y_i$ , since mole fractions are defined as equal to activities in an ideal solution. The chemical reaction and associated equilibrium constant can be used

in determining the relative amounts of each species:



$$K_{\text{eq}} = \{Y_{\text{NaAlO}_2(\text{l})}\}^2 / \{Y_{\text{Na}_2\text{O}(\text{l})} Y_{\text{Al}_2\text{O}_3(\text{l})}\}, \quad (7)$$

much as one would consider a homogeneous, equilibrium mixture of gaseous molecules. More detail is given in Spear et al.<sup>9</sup> with regard to specific energy and activity relationships in this model. The activity values (mole-fraction values) of these species at any given system composition could be inserted into Equation 7 to calculate the value of  $K_{\text{eq}}$  at this temperature. Each system composition would result in the same value of  $K_{\text{eq}}$  for this reaction, since for a given chemical reaction,  $K_{\text{eq}}$  is dependent only on temperature and not composition.

Up to this time, we have set the sum of the nonoxygen atoms in all liquid species equal to two. Empirically better fits of the phase diagrams have been obtained when using two nonoxygen atoms per liquid species rather than one (for example, using the set  $[\text{Na}_2\text{O}(\text{l}), \text{NaAlO}_2(\text{l}), \text{Al}_2\text{O}_3(\text{l})]$  rather than  $[\text{NaO}_{0.5}(\text{l}), \text{Na}_{0.5}\text{Al}_{0.5}\text{O}(\text{l}), \text{AlO}_{1.5}(\text{l})]$ ). Our choice influences the contribution of the ideal mixing energy to the total liquid solution energy, but we have not yet fully developed an understanding of the implications of this observation for the relative structure of the phase diagrams.

Our focus has been on developing accurate thermodynamic data for liquids in binary and ternary subsystems of the HLW glass, since the interactions of oxide species in a complex, multicomponent liquid solution phase will primarily involve two or at most three different constituent metal oxides. For example, the thermodynamic properties of the four-component  $\text{Na}_2\text{O}-\text{Al}_2\text{O}_3-\text{B}_2\text{O}_3-\text{SiO}_2$  liquid solution could be represented by combining the interaction energies of liquid associate species in the binary and ternary subsystems:  $\text{Na}_2\text{O}-\text{Al}_2\text{O}_3$ ,  $\text{Na}_2\text{O}-\text{B}_2\text{O}_3$ ,  $\text{Na}_2\text{O}-\text{SiO}_2$ ,  $\text{Al}_2\text{O}_3-\text{B}_2\text{O}_3$ ,  $\text{Al}_2\text{O}_3-\text{SiO}_2$ ,  $\text{B}_2\text{O}_3-\text{SiO}_2$ ,  $\text{Na}_2\text{O}-\text{Al}_2\text{O}_3-\text{B}_2\text{O}_3$ ,  $\text{Na}_2\text{O}-\text{Al}_2\text{O}_3-\text{SiO}_2$ ,  $\text{Na}_2\text{O}-\text{B}_2\text{O}_3-\text{SiO}_2$ , and  $\text{Al}_2\text{O}_3-\text{B}_2\text{O}_3-\text{SiO}_2$ .

### Phase Diagrams, Thermodynamic Data, and Calculations

Comparisons and optimization of a complete set of thermodynamic data and a phase diagram yield an internally consistent set of thermochemical information for a system. "Fitting of phase diagrams" can always be performed to yield numbers that can be used to "back-calculate"

a phase diagram. However, only if the equations used in the fitting model have a sound thermodynamic basis can the numbers produced be confidently utilized for calculating unstudied regions of the diagram, predicting equilibrium partial pressures and species activities in a system, and modeling more complex chemical systems.

### Calculations for the $\text{Na}_2\text{O}-\text{Al}_2\text{O}_3$ and $\text{Al}_2\text{O}_3-\text{SiO}_2$ Systems

An example of a thermochemically optimized phase diagram is shown in Figure 2 for the  $\text{Na}_2\text{O}-\text{Al}_2\text{O}_3$  binary system.<sup>9,22</sup> The diagram in Figure 2a represents the constant-pressure (1 bar) equilibrium chemical behavior of this system as a function of temperature and composition, showing which phases form when  $\text{Na}_2\text{O}$  and  $\text{Al}_2\text{O}_3$  are mixed in various proportions, melting temperatures and behavior of phases, and solution ranges. Only the liquid phase is shown to exhibit a significant solution in this diagram. Figure 2b depicts the 800°C plot of liquid-species activities as a function of glass composition. This diagram was calculated by suppressing the formation of stable crystalline phases, effectively supercooling the liquid to represent the glass phase. Our liquid solution is represented by an associate-species model, which involves the ideal mixing of end-member constituent liquid species along with an intermediate liquid associate species. Thus the typical excess solution energies of the liquid are included by adding a liquid associate species that has negative formation energies to account for the attractive forces that exist between the end-member constituents. The strong drop in activities of  $\text{Na}_2\text{O}(\text{l})$  and  $\text{Al}_2\text{O}_3(\text{l})$  species with composition seen in Figure 2b is a result of the stable liquid associate species  $\text{NaAlO}_2(\text{l})$ . The liquid is far from being an ideal mixture of  $\text{Na}_2\text{O}(\text{l})$  and  $\text{Al}_2\text{O}_3(\text{l})$ , so that using such an ideal mixture model in describing the leaching behavior of these two end-member constituents would cause errors of many orders of magnitude. The presence of the liquid associate in the ideal solution thus allows a much more accurate calculation of chemical activities.

Figures 3a and 3b show an optimized phase diagram for the  $\text{Al}_2\text{O}_3-\text{SiO}_2$  system,<sup>9,22</sup> and the corresponding 1200°C activity plot for the three supercooled liquid species  $\text{Al}_2\text{O}_3$ ,  $\text{Si}_2\text{O}_4$ , and an associate species  $\{(2/8)\text{Al}_6\text{Si}_2\text{O}_{13}\}$ . In this system, optimizing the phase-diagram and thermodynamic data showed that only weak binary associations occur in the liquid phase. The intermediate associate species

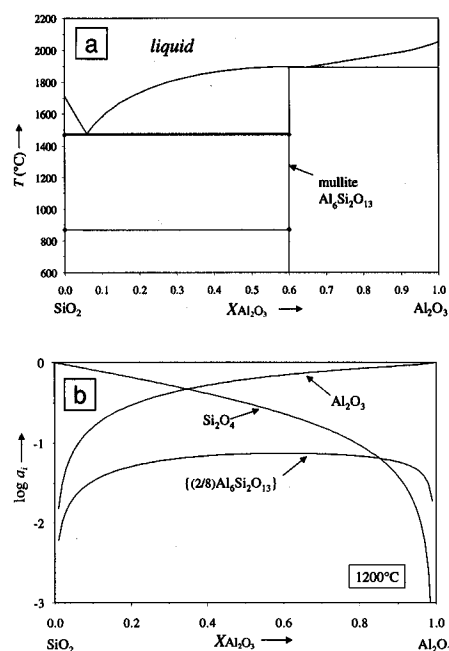


Figure 3. (a) Calculated phase diagram for the  $\text{Al}_2\text{O}_3-\text{SiO}_2$  system using ChemSage<sup>TM</sup>,<sup>3</sup> optimizing the thermodynamic data for the liquid phase to reproduce the melting temperature<sup>5</sup> of the stoichiometric mullite phase. (b) Calculated activities of  $\text{Si}_2\text{O}_4$ ,  $\text{Al}_2\text{O}_3$ , and  $\{(2/8)\text{Al}_6\text{Si}_2\text{O}_{13}\}$  supercooled liquid species at 1200°C for the  $\text{Al}_2\text{O}_3-\text{SiO}_2$  glass system using the thermodynamic data that produced the phase diagram in Figure 3a. The formation of equilibrium crystalline phases was suppressed.

never dominates the liquid phase in this system, indicating that the ideal mixing term contributes significantly to the liquid solution stability at all system compositions.

### Calculations for the $\text{Na}_2\text{O}-\text{B}_2\text{O}_3-\text{SiO}_2$ Systems

Thermodynamic information for the  $\text{Na}_2\text{O}-\text{B}_2\text{O}_3$  system was assessed and optimized by comparisons of reported and calculated binary phase diagrams using the methods outlined in the previous section and in Spear et al.<sup>23</sup> Recent modeling information reported by Hoch<sup>24</sup> for the  $\text{Na}_2\text{O}-\text{B}_2\text{O}_3$  system provided useful initial enthalpies of formation for our optimization process. In general, many of the data for the compound phases had to be estimated or calculated during the optimization process. Our calculated sodium borate phase diagram is shown

in Figure 4 and is a very good representation of the reported phase equilibria for this system. We created an ideal liquid solution phase from liquid components  $\text{Na}_2\text{O}(\text{l})$  and  $\text{B}_2\text{O}_3(\text{l})$ , along with three  $\text{Na}_x\text{B}_y\text{O}_z(\text{l})$  associate liquid species:  $\{(1/3)\text{Na}_4\text{B}_2\text{O}_5\}$ ,  $\text{NaBO}_2$ , and  $\{(1/3)\text{Na}_2\text{B}_4\text{O}_7\}$ . The formation energies for these liquid associate species provide the negative excess free energy of solution that would be needed if only the components  $\text{Na}_2\text{O}(\text{l})$  and  $\text{B}_2\text{O}_3(\text{l})$  were assumed to make up the liquid solution.

The activities of the liquid associate species of  $\text{Na}_2\text{O}$ ,  $\text{B}_2\text{O}_3$ ,  $\{(1/3)\text{Na}_4\text{B}_2\text{O}_5\}$ ,  $\text{NaBO}_2$ , and  $\{(1/3)\text{Na}_2\text{B}_4\text{O}_7\}$  are shown in Figures 5a and 5b for a temperature of  $800^\circ\text{C}$ . Figure 5a shows these liquid species activities when the crystalline compounds are allowed to precipitate, while Figure 5b shows their activities when the liquid is supercooled and crystalline phases are not permitted in the metastable equilibrium. At  $X_{\text{B}_2\text{O}_3}$  compositions greater than 0.3, the  $\text{Na}_2\text{O}(\text{l})$  species activity drops quickly by several orders of magnitude. A similar type of behavior is seen for the  $\text{B}_2\text{O}_3(\text{l})$  activity as compositions move toward the  $\text{Na}_2\text{O}$ -rich part of the diagram. The importance of the intermediate liquid associate species is apparent from their high activities and the subsequent low activities of the end-member  $\text{Na}_2\text{O}$  and  $\text{B}_2\text{O}_3$  species. Calculations of water-leaching of HLW glass components in such a system critically need data such as those shown in Figure 5.

Thermodynamic predictions of glass surface-composition changes that can result from vaporization reactions at high temperatures may be important and are considered for the  $\text{Na}_2\text{O}$ - $\text{B}_2\text{O}_3$ - $\text{SiO}_2$  system. Changes in surface composition

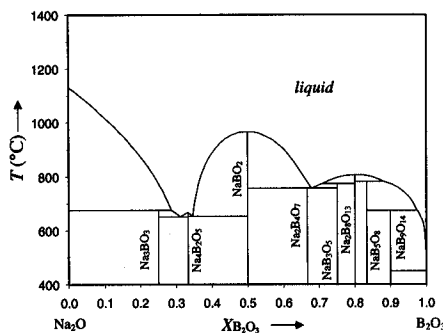


Figure 4. The  $\text{Na}_2\text{O}$ - $\text{B}_2\text{O}_3$  binary phase diagram calculated from an optimized set of thermochemical data.

caused by vaporization losses during high-temperature processing can result in significantly different properties for the bulk and surface of the glass. The result could be leach rates and compatibility with container materials that are quite different for the bulk glass than for

its surface. Such vaporization effects can also be important to many commercial alkali borosilicate-based glass systems.

Calculations of vapor pressures of species in equilibrium with the glass phase were performed as a function of glass composition, temperature, and the partial

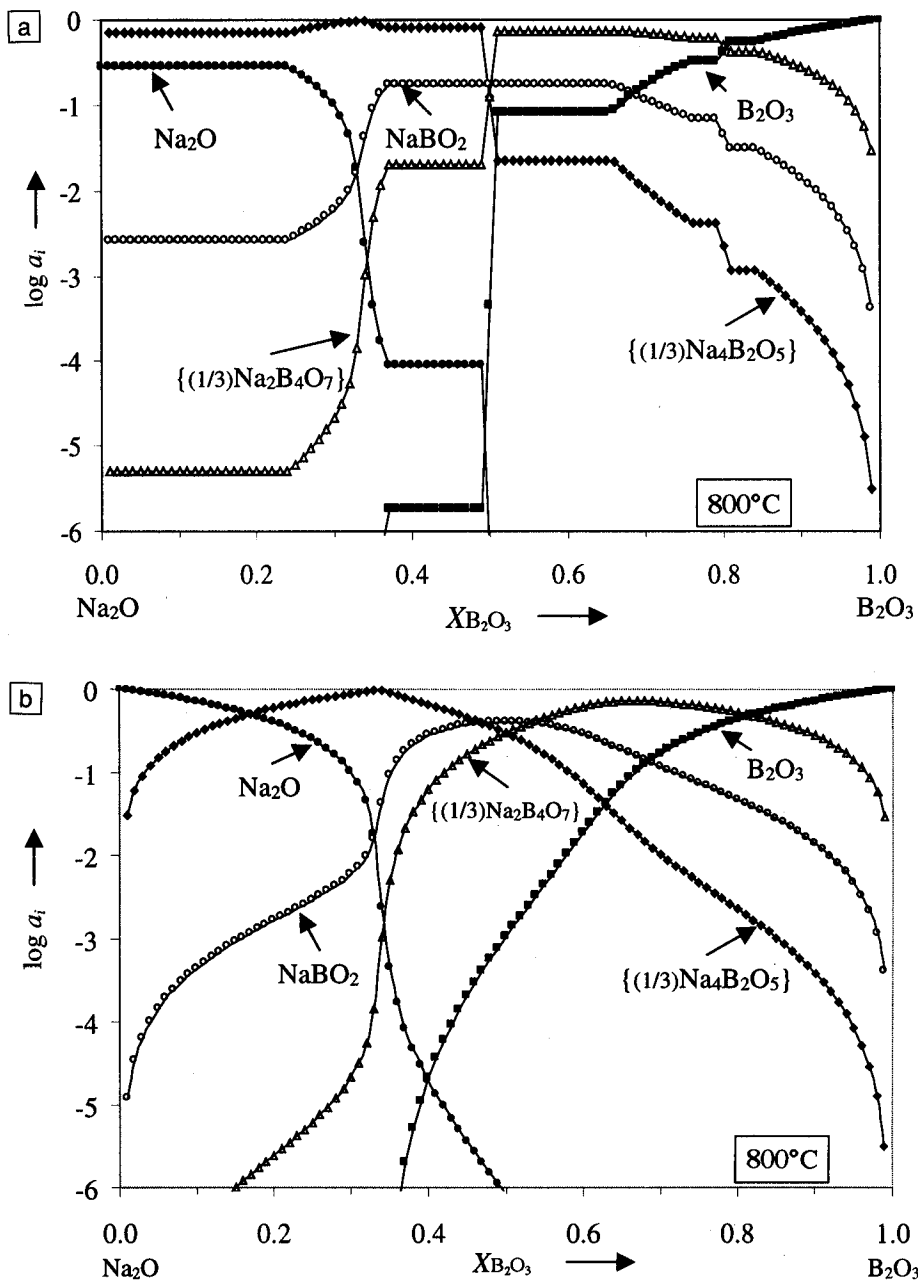
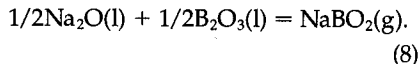


Figure 5. Activities of (a) equilibrium and (b) supercooled liquid (glass) associate species as a function of composition at  $800^\circ\text{C}$  for the  $\text{Na}_2\text{O}$ - $\text{B}_2\text{O}_3$  system. The liquid represented in (a) is in equilibrium with crystalline phases as shown on the diagram in Figure 4. Activities are constant in two-phase equilibrium regions. In (b) crystalline phases are not allowed to equilibrate with the liquid phase. Activities vary continuously with composition in this homogeneous liquid system.

pressures of oxygen and water. Again, these were performed using the computer program ChemSage™, data from the SGTE database,<sup>4</sup> and our assessed data and model for the glass phase.<sup>23</sup> Qualitative changes in surface composition are discussed next, in terms of the preferential vaporization of species containing elements such as boron and alkali metal. Such calculations help pinpoint important variables affecting vapor losses.

Figure 6a shows the equilibrium partial pressures of major gaseous species as a function of temperature above a sodium borate glass with a composition corresponding to that of the crystalline compound  $\text{Na}_2\text{B}_4\text{O}_{13}$ . The activities of the associate species at 800°C are given in Figure 5b at  $X_{\text{B}_2\text{O}_3} = 0.80$ . The oxygen partial pressure was fixed at a value close to that in air. The  $\text{NaBO}_2(\text{g})$  is by far the dominant species, and approaches 1-bar partial pressure around 1300°C. Under such conditions, the surface of this borate glass would quickly become enriched in  $\text{B}_2\text{O}_3$  upon even short exposures to high temperatures. Oxygen pressure has no effect on the  $\text{NaBO}_2(\text{g})$  partial pressure; only the activities of  $\text{Na}_2\text{O}$  and  $\text{B}_2\text{O}_3$  are important, as is seen by the chemical reaction:



Adding  $\text{H}_2\text{O}$  to the system allows for the formation of gaseous species such as  $\text{HBO}_2$ ,  $\text{H}_3\text{BO}_3$ , and  $\text{H}_3\text{B}_3\text{O}_6$ , but their partial pressures never approach that of  $\text{NaBO}_2$ .

Glasses in the  $\text{Na}_2\text{O}-\text{B}_2\text{O}_3-\text{SiO}_2$  system, with B:Si ratios of 1:1 and 1:2, were also examined.<sup>23</sup> Figure 6b shows the partial pressures of major gaseous species for these glass compositions, along with the curves shown in Figure 6a (B:Si = 1:0). In all cases, the Na:B ratio in these glasses was maintained at 1:4, and the oxygen partial pressure at 0.2 bar. No gaseous species involving silicon have significant partial pressures at these temperatures, which means that vaporization losses will cause these glass surfaces to become richer in  $\text{SiO}_2$  than is the bulk. Therefore, the surface of the glass will have decreased  $\text{Na}_2\text{O}$  and  $\text{B}_2\text{O}_3$  activities, and reactions such as leaching involving either of these two species will be diminished.

The additions of  $\text{SiO}_2$  to the sodium borate glass decreases the  $\text{NaBO}_2(\text{g})$  partial pressure by more than an order of magnitude, but appears to have little effect on the boron oxide gaseous species. This is quite understandable, since silica will associate strongly with the  $\text{Na}_2\text{O}$  in

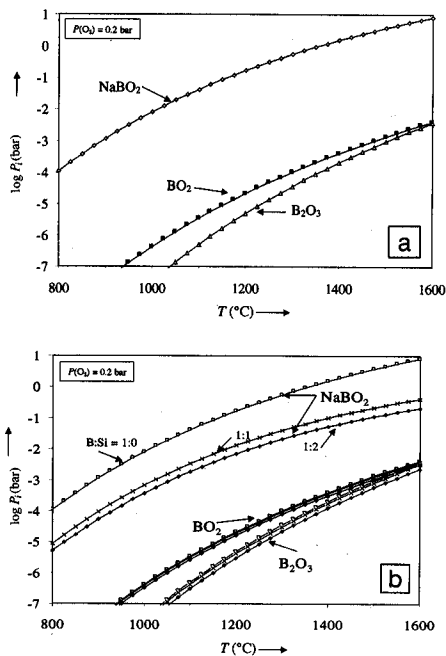


Figure 6. Partial pressures as a function of temperature for the most abundant gaseous species (a) in the glass system with a composition of  $\text{Na}_2\text{B}_4\text{O}_{13}$  and (b) in three  $\text{Na}_2\text{B}_4\text{O}_{13}-\text{SiO}_2$  glass systems. In (a) the glass has a Na:B ratio of 1:4 and a B:Si ratio of 1:0. In (b) the three glasses have a Na:B ratio of 1:4 and respective B:Si ratios of 1:0 (as shown in 6a), 1:1, and 1:2.

the glass, but not with the  $\text{B}_2\text{O}_3$ . Thus, adding silica markedly decreases the activity of  $\text{Na}_2\text{O}$  in Equation 8, but not the activity of  $\text{B}_2\text{O}_3$ . In fact, the association of silica with  $\text{Na}_2\text{O}$  has the effect of increasing the  $\text{B}_2\text{O}_3$  activity over that existing in the initial sodium borate glass. However, dilution of the  $\text{B}_2\text{O}_3$  concentration in the sodium borate glass by adding silica has the opposite effect of lowering the  $\text{B}_2\text{O}_3$  activity. The fact that the  $\text{BO}_2$  and  $\text{B}_2\text{O}_3$  gaseous partial pressures are fairly independent of silica additions indicates that these two effects tend to cancel out.

## Summary

In the efforts to model HLW glass, we have used well-developed estimation techniques and the associate-species model for liquid solutions to obtain internally consistent sets of phase-diagram and thermodynamic data. We have already examined many binary systems in the  $\text{Na}_2\text{O}-\text{Al}_2\text{O}_3-\text{B}_2\text{O}_3-\text{SiO}_2$ ,  $\text{CaO}-\text{MgO}-\text{Al}_2\text{O}_3$ ,  $\text{Al}_2\text{O}_3-\text{TiO}_2-\text{ZrO}_2$ , and  $\text{Li}_2\text{O}-\text{Al}_2\text{O}_3-\text{SiO}_2$  systems, and are well along toward

completing the  $\text{Na}_2\text{O}-\text{Al}_2\text{O}_3-\text{SiO}_2$  and  $\text{Na}_2\text{O}-\text{B}_2\text{O}_3-\text{SiO}_2$  ternary systems. Since our primary interest for the HLW glass is in the liquid and supercooled liquid (glass) solution phases, we are currently not taking into account details of all solid solution phases, but are focusing on optimizing the liquid solution thermodynamic properties. Exceptions such as the complete solid solution of  $\text{NaAlO}_2$  and  $\text{NaAlSiO}_4$  (nepheline) are, however, being included, since the precipitation of nepheline is known to be an important problem in HLW systems.<sup>25</sup> The solubility of other oxides such as  $\text{NaBSiO}_4$  in the nepheline solution phase will also be considered. The precipitation of spinel phases, particularly during high-temperature processing in HLW systems,<sup>26</sup> will also require more detailed modeling of solid solution phases of this structure type. As we gain more experience and insight into applying the associate-species solution model, we will be refining the approach, particularly for systems and phases of critical importance to HLW glass processing and storage.

## Acknowledgments

This research has been supported by the U.S. Department of Energy Environmental Management Science Program, which is funded by the Office of Environmental Management's Office of Science and Technology and administered jointly with the Office of Energy Research under Contract DE-AC05-96OR22464 with Lockheed Martin Energy Research Corporation.

## References

1. A.J.G. Ellison and A. Navrotsky, in *Scientific Basis for Nuclear Waste Management XIII*, edited by V.M. Oversby and P.W. Brown (Mater. Res. Soc. Symp. Proc. 176, Pittsburgh, 1990) p. 193.
2. C.M. Jantzen, in *Corrosion of Glass, Ceramics, and Ceramic Superconductors*, edited by D.E. Clark and B.K. Zaitos (Noyes Publications, Park Ridge, NJ, 1992) p. 153.
3. G. Eriksson and K. Hack, *Metall. Trans. B* 21 (1990) p. 1013; *ChemSage™*, Version 4.1 (GTT Technologies, Herzogonath, Germany, 1998).
4. *SGTE Pure Substance Database*, 1996 Version; produced by the Scientific Group Thermodata Europe and obtained through GTT Technologies (see Reference 3).
5. *Phase Diagrams for Ceramists*, vols. 1-12 (The American Ceramic Society, Westerville, OH, 1964-1996).
6. G. Eriksson, P. Wu, and A.D. Pelton, *CALPHAD* 17 (2) (1993) p. 189.
7. P. Wu, G. Eriksson, and A.D. Pelton, *J. Am. Ceram. Soc.* 76 (8) (1993) p. 2059.
8. G. Eriksson and A.D. Pelton, *Metall. Trans. B* 24 (1993) p. 807.
9. K.E. Spear, T.M. Besmann, and E.C. Beahm,

- in *Proc. High Temperature Corrosion and Materials Chemistry*, vol. 98-9, edited by P.Y. Hou, M.J. McNallan, R. Oltra, E.J. Opila, and D.A. Shores (The Electrochemical Society, Pennington, NJ, 1998) p. 512.
10. K.E. Spear, in *Treatise on Solid State Chemistry*, vol. 4, Chapter 3, edited by N.B. Hannay (Plenum, New York, 1976) p. 115.
  11. J.W. Hastie and D.W. Bonnell, *High Temp. Sci.* **19** (1985) p. 275.
  12. J.W. Hastie, *Pure Appl. Chem.* **56** (1984) p. 1583.
  13. J.W. Hastie, E.R. Plante, and D.W. Bonnell, *Vaporization of Simulated Nuclear Waste Glass* (NIST, Gaithersburg, MD, NBSIR 83-2731, 1983).
  14. D.W. Bonnell and J.W. Hastie, *High Temp. Sci.* **26** (1990) p. 313.
  15. K.E. Spear, P. Benson, and C.G. Pantano, in *High Temperature Materials Chemistry IV*, edited by Z.A. Munir, D. Cubicciotti, and H. Tagawa (The Electrochemical Society, Pennington, NJ, 1988) p. 345.
  16. C.G. Pantano, K.E. Spear, G. Qi, and D.M. Beall, in *Trans. Advances in Ceramic-Matrix Composites*, vol. 38, edited by N. Bansal (The American Ceramic Society, Westerville, OH, 1993) p. 173.
  17. T.E. Paulson, K.E. Spear, and C.G. Pantano, in *Proc. High Temperature Materials Chemistry IX*, vol. 97-39, edited by K.E. Spear (The Electrochemical Society, Pennington, NJ, 1997) p. 194.
  18. *Ibid.*, "Thermodynamic Analysis of the Tin Penetration Profile in High-Iron Float Glass," in *Proc. Int. Congress on Glass, Summer 1998* (The American Ceramic Society, Westerville, OH, 1998).
  19. A.D. Pelton and M. Blander, *Metall. Trans. B* **17** (1986) p. 805.
  20. M. Blander and A.D. Pelton, *Geochim. Cosmochim. Acta* **51** (1987) p. 85.
  21. A.D. Pelton, *Pure Appl. Chem.* **69** (11) (1997) p. 2245.
  22. T.M. Besmann, E.C. Beahm, and K.E. Spear, in *Ceramic Trans. Environmental Issues and Waste Management Technologies in the Ceramic and Nuclear Industries IV*, vol. 93, edited by J.C. Marra and G.T. Chandler (The American Ceramic Society, Westerville, OH, 1999).
  23. K.E. Spear, M.N. Palmisiano, C.G. Pantano, T.M. Besmann, and E.C. Beahm, in *Proc. Fundamental Gas-Phase and Surface Chemistry of Vapor-Phase Materials Synthesis*, vol. 98-23, edited by T.J. Mountziaris, M.D. Allendorf, K.F. Jensen, R.K. Ulrich, M.R. Zachariah, and M. Meyyappan (The Electrochemical Society, Pennington, NJ, 1999).
  24. M. Hoch, *J. Phase Equilibria* **17** (4) (1996) p. 290.
  25. H. Li, J.D. Vienna, P. Hrma, D.E. Smith, and M.J. Schweiger, in *Scientific Basis for Nuclear Waste Management XX*, edited by W.J. Gray and I.R. Triay (Mater. Res. Soc. Symp. Proc. **465**, Pittsburgh, 1997) p. 261.
  26. M. Mika, M.J. Schweiger, J.D. Vienna, and P. Hrma, *ibid.* p. 71. □